

# Spin liquid phase in a $S = 1/2$ quantum magnet on the kagome lattice

S. V. Isakov,<sup>1</sup> Yong Baek Kim,<sup>1</sup> and A. Paramekanti<sup>1</sup>

<sup>1</sup>*Department of Physics, University of Toronto, Toronto, Ontario M5S 1A7, Canada*

(Dated: October 28, 2019)

We study a model of hard-core bosons with short-range repulsive interactions at half-filling on the kagome lattice. Using quantum Monte Carlo (QMC) numerics, we find that this model shows a continuous superfluid to insulator quantum phase transition, with exponents  $z = 1$  and  $\nu \approx 0.67(5)$ . The insulator,  $\mathcal{I}^*$ , exhibits short-ranged density and bond correlations, topological order and exponentially decaying spatial vison correlations, all of which point to a  $Z_2$  fractionalized phase. We estimate the vison gap in  $\mathcal{I}^*$  from the temperature dependence of the energy. Our results, together with the equivalence between hard-core bosons and  $S = 1/2$  spins, provide compelling evidence for a spin-liquid phase in an easy-axis spin-1/2 model with no special conservation laws.

PACS numbers: 75.10.Jm, 05.30.Jp, 71.27.+a, 75.40.Mg

Spin liquid states, or strongly correlated quantum paramagnets that preserve all lattice symmetries, were proposed long ago as plausible candidates for the ground state of frustrated quantum magnets [1]. In recent years, several frustrated antiferromagnets have been discovered which appear to either have a spin-liquid ground state (such as the  $S = 1$  kagome lattice system  $\text{Nd}_3\text{Ga}_5\text{SiO}_{14}$  [2] or the  $S = 1/2$  triangular lattice Mott insulator  $\kappa$ -(ET)<sub>2</sub>Cu<sub>2</sub>(CN)<sub>3</sub> [3]) or are proximate to a spin-liquid phase (such as the  $S = 1/2$  stacked triangular magnet  $\text{Cs}_2\text{CuCl}_4$  [4]), thus lending support to this paradigm. On the theoretical front, there has been considerable progress in understanding the effective field theories and properties of such spin-liquid phases [5, 6, 7, 8], showing that the excitations in this phase carry fractional quantum numbers and interact with emergent gauge fields. However, there is the pressing issue that most microscopic models which can be shown to have a spin-liquid phase have either very unusual interactions [9] or local Hilbert space constraints. An example of the latter are particular triangular [10] and kagome lattice [11] quantum dimer models which have dimer-liquid ground states but are not directly related to any microscopic spin Hamiltonians.

In a significant development, Balents *et al* [12] proposed a model of  $S = 1/2$  spins on the kagome lattice

$$H_{\text{XXZ}} = -J_{\perp} \sum_{\bigcirc} [(S_{\bigcirc}^x)^2 + (S_{\bigcirc}^y)^2 - 3] + J_z \sum_{\bigcirc} (S_{\bigcirc}^z)^2, \quad (1)$$

where  $S_{\bigcirc}^a = \sum_{i \in \bigcirc} S_i^a$  is a sum over the six spins on each hexagon of the kagome lattice unit cell,  $\sum_{\bigcirc}$  denotes a sum over all hexagons on the lattice. This model is easily seen to be a short-range anisotropic XXZ model, with only the first, second and third neighbor interactions being nonzero and equal to each other. Analyzing this model [12] for  $J_{\perp} < 0$  and  $J_z/|J_{\perp}| \gg 1$ , they showed that it directly *maps* onto an effective triangular lattice quantum dimer model with three dimers touching each site. In spin language, this effective model takes the form of a ring-exchange model, with an exchange

scale  $J_{\text{ring}} = J_{\perp}^2/J_z$ , which describes quantum dynamics in the Hilbert space with  $S_{\bigcirc}^a = 0$  on each hexagon (the “dimer subspace”), the local constraint arising from energetic considerations at large  $J_z/J_{\perp}$ . Supplementing this model with an additional four-site (Rokhsar-Kivelson (RK) [13]) potential term of strength  $v_4$  was shown to lead to a spin-liquid for  $v_4 = J_{\text{ring}}$ , which was argued to be stable for small deviations  $v_4 < J_{\text{ring}}$ . Later exact diagonalization (ED) numerics [14] showed that the ring-exchange model appears to be in this spin-liquid phase down to  $v_4 = 0$ , but only modest system sizes (upto 20 unit cells) could be explored. A numerical study of a related rotor model at integer filling on a decorated square lattice [15] also led to a  $Z_2$  spin liquid, but the corresponding  $S = 1/2$  model has not been studied.

In this paper, we show the presence of a spin-liquid phase in a  $S = 1/2$  model on the kagome lattice, by studying numerically the Hamiltonian (1) with  $J_{\perp} > 0, J_z > 0$ . Since the ring-exchange model is independent of the sign of  $J_{\perp}$ , we expect to recover the physics of the ring-exchange model at large  $J_z$ , but without any Hilbert space restrictions. On the technical side, the choice of  $J_{\perp} > 0$  eliminates the QMC sign problem. This permits us to study very large systems at very low temperature using a generalized stochastic series expansion (SSE) QMC algorithm [16, 17] and, thus, to go significantly beyond earlier work on this class of models.

By the mapping between  $S = 1/2$  spins and hard-core bosons, model (1) is equivalent to a hard-core boson model at half-filling

$$H_b = -t \sum_{(i,j)} (b_i^{\dagger} b_j + \text{H.c.}) + V \sum_{\bigcirc} (n_{\bigcirc})^2 - \mu \sum_i n_i, \quad (2)$$

where  $b_i^{\dagger}(b_j)$  is the boson creation(annihilation) operator,  $t = J_{\perp} > 0$  is the boson hopping amplitude,  $V = J_z > 0$  is the boson repulsion strength,  $n_i = b_i^{\dagger} b_i$  is the boson number operator, and  $\mu = 12J_z$  is the chemical potential. The hopping term connects only the first, second and third neighbors. We begin by showing that model (2) exhibits a superfluid-insulator transition at  $(V/t)_c \approx 19.8$ .

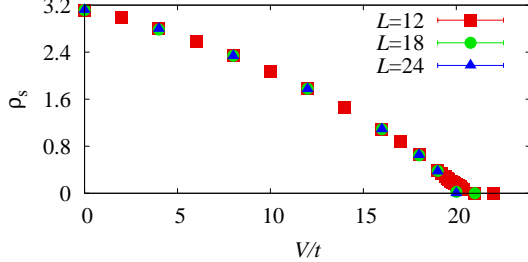


FIG. 1: (color online). The superfluid density  $\rho_s$  versus  $V/t$ , at  $T = t/9$  for different linear system sizes  $L$ . Finite-size effects, significant only near the quantum phase transition, are discussed in the text and Fig. 2.

We then turn to the nature of the insulating phase and show that it is a topologically ordered  $Z_2$  Mott insulator. We thus arrive at the result that for  $J_\perp > 0$ , model (1) exhibits a ferromagnetic phase at small  $J_z$  and a  $Z_2$  fractionalized spin-liquid at large  $J_z$ , separated by a continuous quantum phase transition at  $(J_z/J_\perp)_c \approx 19.8$ .

*Superfluid-insulator transition.*—For small values of  $V/t$ , we expect the ground state of (2) to be a superfluid ( $\mathcal{SF}$ ). We confirm this by measuring the superfluid density  $\rho_s$  through winding number fluctuations  $W_{a_{1,2}}$  [18] in each of the two lattice directions, with  $\rho_s = (1/2\beta t)(\langle W_{a_1}^2 \rangle + \langle W_{a_2}^2 \rangle)$ , where  $\beta$  is the inverse temperature. As seen from Fig. 1, for small  $V/t$ ,  $\rho_s$  is large (its value agrees with mean field estimates [19]). The superfluid density decreases with increasing  $V/t$ , eventually vanishing for  $V/t \gtrsim 20$  suggesting a phase transition to an insulating phase ( $\mathcal{I}^*$ ). This behavior is in sharp contrast to a nearly identical model where the hopping and repulsive interactions are restricted to the nearest neighbor only — in that case a uniform superfluid persists for arbitrarily large  $V/t$  [20]. The absence of a jump in  $\rho_s$  in Fig. 1 suggests that the  $\mathcal{SF} - \mathcal{I}^*$  transition is continuous.

In the vicinity of a continuous phase transition, the superfluid density should scale as  $\rho_s = L^{-z} F_{\rho_s}(L^{1/\nu}(K_c - K), \beta/L^z)$ , where  $F_{\rho_s}$  is the scaling function,  $L$  is the linear system size,  $z$  the dynamical critical exponent,  $\nu$  the correlation length exponent, and  $(K_c - K) \propto (V_c - V)/t$  is the distance to the critical point. Thus if we plot  $\rho_s L^z$  as a function of  $V/t$  at fixed aspect ratio  $\beta/L^z$ , the curves for different system sizes should intersect at the critical point. The inset of Fig. 2 shows such a plot for  $z = 1$  and  $\beta/L = 3/(4t)$  with a clear crossing point at  $(V/t)_c \approx 19.8$ . The data is thus consistent with a continuous  $\mathcal{SF} - \mathcal{I}^*$  transition with the dynamical exponent  $z = 1$ . To obtain the correlation length exponent  $\nu$ , we plot  $\rho_s L$  as a function of  $[(V/t)_c - V/t]L^{1/\nu}$  for different system sizes. It follows from the above scaling relation that the curves for different system sizes should collapse onto a universal curve  $F_{\rho_s}$  for a properly chosen  $(V/t)_c$  and  $\nu$ . In Fig. 2, we show such a data collapse for  $(V/t)_c = 19.80(2)$  and  $\nu = 0.67(5)$ . The error bars are estimated from the sta-

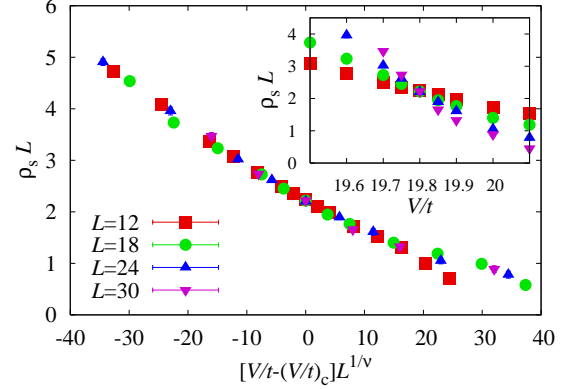


FIG. 2: (color online). Data collapse of the superfluid density  $\rho_s$  for  $\beta/L = 4/(3t)$ ,  $(V/t)_c = 19.80(2)$ , and  $\nu = 0.67(5)$ . Inset: Finite size scaling of  $\rho_s$  for  $\beta/L = 4/(3t)$ .

bility of the collapse towards varying the parameters. To summarize, we find a  $\mathcal{SF} - \mathcal{I}^*$  transition with exponents  $z = 1$  and  $\nu = 0.67(5)$ . We next examine the nature of the insulator  $\mathcal{I}^*$ .

*$\mathcal{I}^*$  does not break lattice symmetries.*—For a system of bosons, generalizing a flux-threading argument of Oshikawa [21] shows that that an insulating state at half-filling could either be a conventional state with broken lattice symmetries or must *necessarily* have topological order [22] (which means the ground state degeneracy depends on the topology of the system). We rule out the first possibility here by studying correlation functions in the insulating state. We look for signatures of diagonal (density) ordering by studying the equal-time density structure factor  $S(\mathbf{q})/N = \langle \rho_{\mathbf{q}\tau}^\dagger \rho_{\mathbf{q}\tau} \rangle$ , where  $\rho_{\mathbf{q}\tau} = (1/N) \sum_i \rho_{i\tau} \exp(i\mathbf{q}\mathbf{r}_i)$  and  $\rho_{i\tau}$  is the boson density at site  $i$  and imaginary time  $\tau$ . Fig. 3 compares a contour plot of the equal time structure factor to that of the classical model (with  $J_\perp = 0$ ) which is known to have short-range correlations [23]. The striking similarity between the two suggests short-ranged density correlations in the full quantum ground state of the insulator. We confirm this via a careful examination of the equal-time structure factor on large system sizes. Upto  $L = 48$  we do not find any Bragg peaks which rules out the possibility of density ordering even with moderately large unit cells. We also examine for possible bond ordering in  $\mathcal{I}^*$  by computing the bond-bond structure factor  $S_b(\mathbf{q})/N = \langle B_{\mathbf{q}\tau}^\dagger B_{\mathbf{q}\tau} \rangle$ , where  $B_{\mathbf{q}\tau} = (1/N) \sum_\alpha B_{\alpha\tau} \exp(i\mathbf{q}\mathbf{r}_\alpha)$  is summed over the bond index  $\alpha$  connecting spins  $i$  and  $j$ , and  $B_{\alpha(i,j),\tau} = t(b_i^\dagger b_j + b_i b_j^\dagger)$  is the off-diagonal bond operator. Again, we find no signatures of ordering from the bond-bond structure factor.

Finally, the  $\mathcal{SF} - \mathcal{I}^*$  transition appears to be continuous rather than first-order which would be expected if we had a conventional transition between a superfluid and a broken symmetry insulator. This argument, together with the correlation function results, strongly fa-

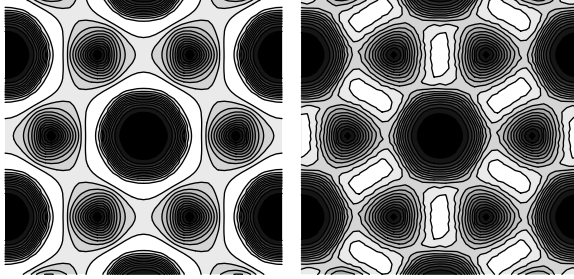


FIG. 3: Contour plots of the equal-time density structure factor for the classical model (with  $t=0$ ) [23] (left panel) for  $L = 24, T = 0$  and in the quantum insulator (right panel) for  $L = 24, V/t = 20, T = t/12$ . In both panels the axes range from  $-2\pi$  to  $2\pi$ .

vor a non-broken-symmetry ground state for  $\mathcal{I}^*$ . Therefore, we next examine the second possibility, that  $\mathcal{I}^*$  is a featureless topologically ordered Mott insulator (a ‘spin-liquid’ in magnetic language).

*Topological order in  $\mathcal{I}^*$ .*—On a lattice with periodic boundary conditions in both lattice directions, the subspace of configurations with  $n_{\bigcirc} = 3$  on every kagome hexagon (the “dimer subspace” which dominates the boson wavefunction for  $V \rightarrow \infty$ ) has topological sectors defined by having, for each lattice direction  $a_{1,2}$ , an odd (or even) number of bosons on each row (so-called parity sectors). In this torus geometry and in the restricted Hilbert space, we thus find four topological sectors labelled by row and column parity, such that any local move which obeys the local constraint  $n_{\bigcirc} = 3$  leaves the sector unchanged. In order to change from one sector to another one needs to make highly nonlocal boson moves over loops which wind around the lattice.

The row/column parities are however not well-defined in model (2) since at any finite  $V$ , no matter how large, there will be a small density of hexagons with  $n_{\bigcirc} \neq 3$  [24]. We have checked in our numerics, where we start from a configuration in the dimer subspace with a certain row/column parity, that the QMC algorithm generates a small density of particle-hole pair defects in equilibrium, so that the quantum ground state no longer lies in the “dimer subspace”. However, for a large enough system size at a given value of  $V/t$  ( $L \gtrsim 10$  at  $V/t = 26$ ), we find that our simulations with the longest accessible MC steps do not lead to any non-local boson moves which wind around the lattice. Thus the winding number identically vanishes, and each configuration in the simulation which lies in the dimer subspace belongs to the same parity sector as the initial configuration. The full ground state accessed by the QMC is, in this sense, perturbatively connected to the initial parity sector, consistent with the charge gap in the insulating state. This means that four topological sectors continue to exist in this case, and we can label them simply by the row/column parity of that component of the ground state wavefunction which lies

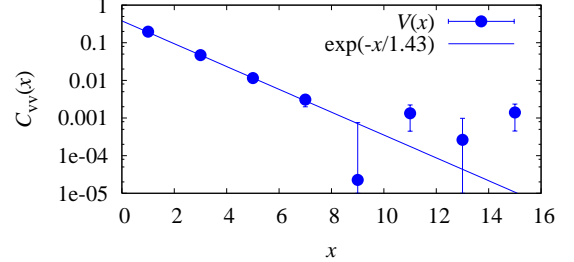


FIG. 4: (color online). Equal-time vison-vison correlation function for  $L=24$  and  $T=t/18$  in the insulator at  $V/t=20.5$ , showing exponential decay with a length scale  $\xi=1.43(5)$ .

in the dimer subspace.

For a *topologically ordered* insulator, the ground state energy should be *identical* in each of the four topological sectors (on a torus) leading to a ground state degeneracy of four. We have computed the energy of the four ground states by starting our simulations from configurations in the dimer subspace lying in four different parity sectors. We find that they are equal within statistical errors, which is strong evidence for topological order [25].

*Spatial vison correlations in  $\mathcal{I}^*$ .*—A second signature of  $Z_2$  fractionalization is that visons, which are gapped  $Z_2$  vortices in the effective field theory description, should have exponentially decaying spatial correlations. While visons are point-like excitations when viewed as localized vortices, they are highly nonlocal operators in terms of the original particle operators. The spatial vison-vison correlation function is thus the expectation value of a string operator. For the ring-exchange model (valid for  $V/t \rightarrow \infty$ ), it takes the form [12]

$$C_{vv}(r_{ij}) = \left| \langle 0 | \prod_{k=i}^j e^{i\pi n_k} | 0 \rangle \right|, \quad (3)$$

where  $|0\rangle$  denotes the ground state and the product is along some path on the kagome lattice that contains an even number of sites, starts at site  $i$ , and ends at site  $j$ , making only “ $\pm 60^\circ$ ” turns to the left or right. The boson number  $n_k$  at site  $k$  takes values 0, 1 due to their hard-core nature. The absolute value of the product in Eq. (3) is *path-independent* in the dimer subspace, and it is expected to decay exponentially in the topologically ordered phase. In model (1) at finite  $V/t$ , ground state no longer lies entirely in the dimer subspace, but will mix in configurations with particle-hole defects. Correspondingly, the vison operator must include correction terms to the above definition since it otherwise becomes path-dependent in the presence of such defects. Both, the corrected ground state wavefunction and the vison operator, may be determined order-by-order in a perturbation expansion [19], undoing the unitary transformation that leads from model (2) to a ring-exchange Hamiltonian.

Here we content ourselves with evaluating the leading

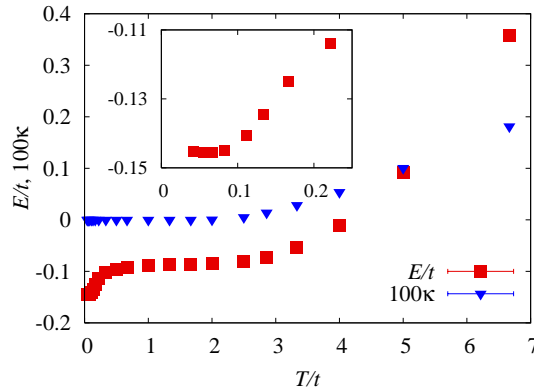


FIG. 5: (color online). Energy per site  $E$  and compressibility  $\kappa$  versus temperature for  $L = 24$  ( $V/t = 20.5$ ). The energy rises exponentially at very low  $T$  (see inset) with a wide intermediate plateau from  $T/t \sim 0.5 - 3$  (see text). The compressibility is zero (within error bar) at low  $T$ , rising only at  $T \sim 3t$  once gapped charge (spinon) excitations become relevant.

term, correct to  $\mathcal{O}(t/V)$ , of the vison-vison correlation function, which is obtained [19] by computing the above string expectation value in Eq. 3 in the true ground state *projected into the dimer subspace*. As seen from Fig. 4, the vison-vison correlation function decays exponentially in  $\mathcal{I}^*$ , with the signal at large distances becoming comparable to the error bars, again signaling topological order in  $\mathcal{I}^*$ . We estimate a ‘decay length’,  $\xi = 1.43(5)$ , which is comparable to its value at the RK point of the ring-exchange model [12],  $\xi \approx 1$ , and to that found by ED [14],  $\xi \approx 1.7$ , in the ring-exchange model with  $v_4 = 0$ .

*Vison gap.*—To provide further evidence for gapped vison excitations, we display the temperature dependence of the system energy per site and compressibility  $\kappa = \frac{\beta}{N} \langle (\sum_i n_i)^2 \rangle$  in Fig. 5. The energy exhibits a two-step decrease upon lowering temperature, with a distinct intermediate plateau, before vanishing exponentially at a very low temperature. We identify the first drop in energy with a freezing out of charge fluctuations below a charge gap scale, which we confirm by the sharp decrease in compressibility at this temperature (also shown in Fig. 5). The plateau then corresponds to a regime where the system dominantly explores configurations with  $n_{\text{hexagon}} = 3$  on each hexagon. (The large difference between the total energy of the ground state and that in the plateau regime can be explained by the macroscopic entropy density of multiple vison excitations [19].) Finally at the lowest temperature, the system begins evolving into the spin-liquid ground state. Heating up from  $T = 0$ , we therefore identify the lowest energy excitations out of the ground state as vison-pair excitations (since the charge gap is much larger). The temperature dependence of the energy then leads to a rough estimate of the single vison gap  $E_v/t \sim 0.35(15)$ .

*Conclusions.*—To summarize, we have studied the zero

temperature phase diagram of a hard-core boson model with short-range repulsion on the kagome lattice using QMC numerics. We find a continuous transition from a superfluid phase to a featureless Mott insulator with increasing repulsion. In magnetic language, this corresponds to a ferromagnet-paramagnet transition with the paramagnet being a correlated quantum spin-liquid. This spin-liquid supports gapped visons and exhibits topological order characteristic of a  $Z_2$  fractionalized phase. The apparently 3D XY exponents at the  $\mathcal{I}^* - \mathcal{SF}$  transition,  $z = 1$  and  $\nu = 0.67(5)$ , are consistent with superfluidity emerging from the insulator by condensation of fractionalized charge-1/2 bosons [15]. We have estimated the vison gap in the spin liquid from the temperature dependence of the energy. Two final points need to be mentioned. The spin liquid phase in our model is fully gapped and thus stable to weak perturbations away from the special choice of exchange couplings in our model. Although our model is not of direct relevance to known magnetic materials, our study is nevertheless important in showing a spin liquid phase in a model with purely local interactions and no special conserved quantities. It thus represents significant progress in the direction of understanding realistic Hamiltonians with spin liquid ground states.

This work was supported by the CRC, CIAR, NSERC of Canada, and KRF2005-070-C00044 (SVI, YBK). We thank L. Balents and D.-N. Sheng for useful discussions.

---

- [1] P. Fazekas and P. W. Anderson, Phil. Mag. **30**, 423 (1974).
- [2] J. Robert, *et al*, Phys. Rev. Lett. **96**, 197205 (2006).
- [3] Y. Shimizu, *et al*, Phys. Rev. Lett. **91**, 107001 (2003).
- [4] R. Coldea, *et al*, Phys. Rev. Lett. **86**, 1335 (2001).
- [5] X. G. Wen, Phys. Rev. B **44**, 2664 (1991) and Cargese Lectures (1990, unpublished).
- [6] S. Sachdev, Phys. Rev. B **45**, 12377 (1992).
- [7] T. Senthil and M. P. A. Fisher, Phys. Rev. B **62**, 7850 (2000).
- [8] O. I. Motrunich and T. Senthil Phys. Rev. B **71**, 125102 (2005).
- [9] A. Kitaev, cond-mat/0506438 (unpublished); X.-G. Wen, Phys. Rev. Lett. **90**, 016803 (2003).
- [10] R. Moessner and S. L. Sondhi, Phys. Rev. Lett. **86**, 1881 (2001).
- [11] G. Misguich, D. Serban and V. Pasquier, Phys. Rev. Lett. **89**, 137202 (2002).
- [12] L. Balents, M. P. A. Fisher, and S. M. Girvin, Phys. Rev. B **65**, 224412 (2002).
- [13] D. S. Rokhsar and S. A. Kivelson, Phys. Rev. Lett. **61**, 2376 (1988).
- [14] D. N. Sheng and L. Balents, Phys. Rev. Lett. **94**, 146805 (2005).
- [15] T. Senthil and O. Motrunich, Phys. Rev. B **66**, 205104 (2002); Phys. Rev. Lett. **89**, 277004 (2002).
- [16] A. W. Sandvik, Phys. Rev. B **59**, R14157 (1999); O. F.

Syljuåsen and A. W. Sandvik, Phys. Rev. E **66**, 046701 (2002).

[17] Since the standard algorithm based on a bond as the elementary lattice unit is not very efficient at large  $J_z/J_{\perp}$ , we use a plaquette generalization (see K. Louis and C. Gros, Phys. Rev. B **70**, 100410 (2004)), where the elementary lattice unit is a kagome hexagon.

[18] E. L. Pollock and D.M Ceperley, Phys. Rev. B **36**, 8343 (1987).

[19] S. Isakov, Y.-B. Kim and A. Paramekanti (unpublished).

[20] S. V. Isakov, *et al*, Phys. Rev. Lett. **97**, 147202 (2006).

[21] M. Oshikawa, Phys. Rev. Lett. **84**, 1535 (2000).

[22] A. Paramekanti and A. Vishwanath, Phys. Rev. B **245118** (2004).

[23] K. Gregor, S. V. Isakov, R. Moessner, S. L. Sondhi, (unpublished).

[24] Such defects correspond to particle-hole pairs in real space, which are necessarily bound to each other since the system is insulating and charges cannot propagate freely in the ground state.

[25] For a finite size system which becomes a topologically ordered insulator in the thermodynamic limit we expect four *nearly* degenerate ground states with an energy splitting (arising from nonperturbative effects, e.g., vison tunneling) which is exponentially small in linear system size. Evaluating this splitting is beyond the scope of our QMC simulations.